

論文 / 著書情報
Article / Book Information

Title	Organic double layer element driven by triboelectric nanogenerator: Study of carrier behavior by non-contact optical method
Authors	Xiangyu Chen, Dai Taguchi, Takaaki Manaka, Mitsumasa Iwamoto, Zhong Lin Wang
Citation	Chemical Physics Letters, 646, 64-68
Pub. date	2016, 1
DOI	http://dx.doi.org/10.1016/j.cplett.2016.01.002
Creative Commons	See next page.
Note	This file is author (final) version.

License



Creative Commons: CC BY-NC-ND

Organic double layer element driven by triboelectric nanogenerator: study of carrier behavior by non-contact optical method

Xiangyu Chen¹, Dai Taguchi², Takaaki Manaka², Mitsumasa Iwamoto^{2*}

1. *Beijing Institute of Nanoenergy and Nanosystems, Chinese Academy of Sciences,
Beijing 100083, China,*

2. *Department of Physical Electronics, Tokyo Institute of Technology,
2-12-1 S3-33 O-okayama, Meguro-ku Tokyo 152-8552 Japan*

E-mail: chenxiangyu@binn.cas.cn, iwamoto@pe.titech.ac.jp

By using optical electric-field-induced second-harmonic generation (EFISHG) technique, we studied carrier behavior caused by contact electrification (CE) in an organic double-layer element. This double-layer sample was half suspended in the open air, where one electrode (anode or cathode) was connected with a Cu foil for electrification while the other electrode was floated. Results showed two distinct carrier behaviors, depending on the (anode or cathode) connections to the Cu foil, and these carrier behaviors were analyzed based on the Maxwell-Wagner model. The double-layer sample works as a simple solar cell device. The photovoltaic effect and CE process have been proved to be two paralleled effects without strong interaction with each other, while photoconductivity changing in the sample can enhance the relaxation of CE induced charges. By probing the carrier behavior in this half-suspended device, the EFISHG technique has been demonstrated to be an effective non-contact method for clarifying the CE effect on related energy harvesting devices and electronics devices. Meanwhile, the related physical analysis in this letter is also useful for elucidating the fundamental characteristic of hybrid energy system based on solar cell and triboelectric nanogenerator.

Keywords: EFISHG, OSCs, contact electrification, charge injection.

1. Introduction

For the basic study and the application of electronics devices, electrostatic interference caused by contact electrification (CE) is a serious problem, which must be removed. However, in the last 4 years, a newly introduced technique, triboelectric nano-generator (TENG), using CE process and electrostatic induction for collecting electrical energy, has found useful applications as hybrid power source, self-powered sensors and so on [1-4]. Among these applications, solar cell devices also have been integrated with TENG device to collect energy from both solar and various tribo-motions, such as rain drops or wind motion [5-7]. The good compatibility of nanogenerator can allow this kind of devices to be integrated with various electronics system [8, 9]. Even though the validity of this kind of hybrid energy harvesting system has been fully demonstrated, the detailed study about the contact-electrified carrier behavior inside the integrated electronics devices has not been fully established yet. CE effect is a strong instantaneous process, while its performance can be easily influenced by environmental conditions or by the detecting instrument itself [6, 9]. Hence, the detailed carrier behavior inside the devices integrated with TENG cannot be easily elucidated by using the conventional electrical methods. The electronic device hybridized with TENG usually shows distinct performance in comparison with the conventional devices driven by stable power supply [4, 6, 8]. It is thus necessary to employ a detecting method with high experimental flexibility for this kind of study, in order to isolate the electrostatic interference.

In our previous studies, by using optical electric-field-induced second-harmonic generation (EFISHG) measurement, we analyzed photo-induced interfacial carrier behaviors of organic solar cells (OSCs) [10, 11]. The experimental flexibility of this optical method allowed us to investigate fundamental carrier processes in OSCs [11, 12], without being influenced by electrostatic interference. These research progresses motivated us to study the detailed carrier behaviors in a hybrid energy generating system of both OSCs and TENG. In this study, we employed an organic double-layer element and a single-electrode TENG to form a simple hybrid energy harvesting system. We designed a half-suspended electrode configuration for this organic sample, where one of the electrodes was floating in the open air (electrically isolated), and the other electrode was connected with a Cu foil. This half-suspended structure, where the energy from moving objects is collected, is a key to understand carrier mechanism of hybrid energy generating systems [3-5]. A conventional electrical instrument such as a voltage meter is not sufficient to study half-suspended electrode system since the system need to be electrically isolated. On the other hand, the EFISHG is capable of directly probing carrier processes without electrical connection, and it can be helpful for studying carrier process in these devices. Hence, by using the optical EFISHG

technique, the carrier behaviors triggered by CE effect inside this hybrid energy system were studied in a non-contact situation. The experimental study and the analysis based on the Maxwell-Wagner model showed the working mechanism of electronics devices under CE excitation, and elucidated the contribution of open air during the CE. These results are helpful for further development of hybridized energy system with TENG and photovoltaic devices.

2. Experiments

Double-layer elements with an IZO/pentacene (50 nm)/C₆₀ (60 nm)/Al structure were prepared as portrayed in Fig. 1(a). The working area of the electrodes was $A = 3.1 \text{ mm}^2$. Prepared elements were sealed in a dry bottle to prevent the degradation, while the current-voltage (I-V) and EFISHG measurements were conducted in the laboratory atmosphere. A red light (wavelength 630 nm, intensity 1 mW/cm²) was used as a light source to provide illumination source [10, 11]. Figure 1 (b) shows the I-V characteristics of this double-layer element under illumination and in the dark. This element showed a photovoltaic effect, where the open-circuit voltage V_{oc} was 0.22 V, the short-circuit current density J_{sc} was -0.23 mA/cm², and the fill factor was 0.15. The photovoltaic performance of this element as organic solar cell was quite low, but this structure is suitable for studying the fundamental physical process induced by CE. The similar research approach has been demonstrated to be effective in the previous studies [10-12]. Figure 1 (c) shows the Maxwell-Wagner type equivalent circuit of the double-layer element [10, 11]. Here C_i ($i=1, 2$) and G_i ($i=1, 2$) represent capacitance and conductance of pentacene ($i = 1$) and C₆₀ ($i = 2$), respectively. The prepared double-layer element is half suspended in the open air, while either IZO electrode or Al electrode is connected to a Cu foil with a size of 4 cm × 6 cm, as portrayed in Fig. 1(a). The Cu foil is used as the input terminal for the CE effect, while another polyimide film with a thickness of 50 μm is contacted with the Cu foil to induce static electric field. The contact and separation speed is controlled to be 0.05 m/s. Hence, the separation motion is a very fast process and it takes about 0.6 s. After the separation, the waiting time between contact and separation motion is about 2 second. This waiting time is applied for EFISHG signal to observe the carrier migration and the interfacial charge relaxation inside the pentacene/C₆₀ double-layer element. In order to obtain the detailed quantitative analysis as the Maxwell-Wagner element under the excitation of TENG, we can employ finite element method to simulate the output of the TENG and solve the differential equation based on the Maxwell-Wagner model, as we did in the previous study [13]. The purpose of the Maxwell-Wagner model is to help us better understand the effect of charge accumulation (Q_s) at the interface. It is necessary to note that the electrostatic field across the sample is sum of the external electrical field and the space charge field

originated from interfacial charges. That is why Maxwell-Wagner model is more suitable for this study. Meanwhile, for simplifying the analysis, this Maxwell-Wagner model can be transformed into a unified form, where a capacitor and a conductor were connected in paralleled structure (see Fig. S1 in supplemental material [22]). The related analysis of this unified model is similar to the previous studies of our colleagues [14, 15].

According to our previous study, polyimide surface is negatively charged by the CE effect with metal foil [16, 17], while the Cu foil as well as the connected electrode are positively charged. The output voltage from Cu foil in connection with double-layer element is also checked by using a Keithley multimeter, as shown in Fig. 1(a). Figure 1(a) also shows the laser arrangement used for the EFISHG measurements [10, 11]. We used a laser beam with a wavelength of $\lambda_{\omega}=1,000$ nm, and recorded the generated EFISHG signal at a wavelength of $\lambda_{2\omega}=500$ nm to selectively measure the electric field in C_{60} layer [11, 12]. The generated EFISHG signal was due to the coupling of electrons in C_{60} molecules and the electric field of incident laser beam $E(\omega)$ in the presence of local electrostatic field $E(0)$ in the C_{60} layer, and the square-root of the SHG signal I_{SHG} was in proportion to the electric field $E(0)$ with the relation $I_{SHG} \propto |E(0)|^2$ [18, 19].

3. Results and discussion

For solar cell system hybridized with TENG, one of the two electrodes is usually suspended in air to contact with moving objects for generating electricity [3-5]. Therefore, the contribution of the open air to the carrier behavior should be studied. Figures 2(a) and (b) show the EFISHG results from the contact-excited double-layer elements, where the sample was half suspended and the Cu foil was connected to the IZO electrode (IZO-Cu connection) and the Al electrode (Al-Cu connection), respectively. The optical EFISHG measurements were carried out in the way similar to the conventional electrostatic measurement, with a sampling rate of 0.1 s. The response of the EFISHG signal showed distinctly different behaviors, as shown in Figs. 2(a) and (b). For the IZO-Cu connection (see Fig. 2(a)), one peak was observed during both separation and contact motions, indicating that carrier accumulation and relaxation happened successively in the device. On the other hand, for the Al-Cu connection (see Fig. 2(b)), the EFISHG response was stable, nearly constant, during both separation and contact motions, suggesting that the CE effect never influences the carrier behaviors in the device. It is necessary here to point out that the two different carrier behaviors in Figs. 2(a) and (b) can only be observed by using the EFISHG measurement. The electrical instruments, such as multimeters, have their internal grounded end and therefore the OSCs studied by using multimeters are actually under grounded state. Hence, the carrier behavior observed using

a multimeter will be totally different, as can be seen in Fig. S2 in supplemental material [22]. Noteworthy that using the relationship of $I_{SHG} \propto |E(0)|^2$, the EFISHG intensity was directly transferred into electric field strength based on the relationship of $\sqrt{I_{SHG}} \propto |E(0)|$ [18, 19]. As shown in Fig. S3(a), we firstly performed the EFISHG measurement with applied DC step voltage ($V_{ex} = \pm 1$ V), in order to normalize the conversion ratio between SHG intensity and electrostatic field. Figure S3(a) shows the transient interfacial charging processes of the double-layer OSCs in dark, in response to the DC step voltage pulse (± 1 V, 10 Hz). The detailed explanation related to this measurement has been well analyzed in previous researches on bias of Maxwell-Wagner effect [10-12]. From the Fig. S3(a), the normalized relationship between the changing of the $\sqrt{I_{SHG}}$ and the changing of the electric field in C₆₀ layer is obtained, where 1 unit of the changing of $\sqrt{I_{SHG}}$ is related to the electric field of 0.47×10^7 V/m. By using this obtained relationship [12], the EFISHG signal shown in Fig. 2(a) was rescaled to be the electric field strength, as can be seen in Fig. S3(b). These results can help us to better understand the probed intensity changing of the SHG signal.

The external field generated by the CE is given as $E_{ex} = \frac{C_1}{C_1 + C_2} \frac{V_{ex}}{d_2}$, where V_{ex} is the voltage generated by the CE across the double-layer element. On the other hand, the Maxwell-Wagner model illustrated in Fig. 1(c) accounts for the presence of space charge field E_s induced across the C₆₀ layer (layer $i=2$), due to the accumulated interfacial charge Q_s , and it is given by $E_s = \frac{Q_s}{C_1 + C_2} \frac{1}{d_2}$. Therefore the local electric field $E(0)$ in the C₆₀ layer is given as the sum of these two electric fields, $E_{ex} + E_s$ [10, 11]. According to the Maxwell-Wagner model, the charge Q_s accumulates at the interface between pentacene and C₆₀, because the dielectric relaxation times (given by $\tau = \varepsilon/\kappa$, ε : dielectric constant, κ : conductivity) are different between pentacene and C₆₀. Accordingly, the current flow induced by the CE makes a significant contribution to the EFISHG response. The sharp increase and decrease of EFISHG signal observed in Fig. 2(a) traces the establishment of $E_{ex} + E_s$, along with the CE process. That is, in response to the separation of polyimide film from the Cu-foil, the CE-excited positive charges on Cu foil are injected into the half suspended double-layer elements and then accumulated at the interface between pentacene and C₆₀. From viewpoints of equivalent electrical circuit analysis, an imaginary grounded cathode can be applied to describe the effect of the CE, as shown in Fig. 2(c). This imaginary grounded cathode is to support the model of hole injection followed by hole transport across the pentacene layer. That is, the contact-generated holes are allowed to be injected into OSC and then transported to the Al electrode, in a way

suggested by the equivalent circuit with a grounded cathode. This possible mechanism is illustrated as an imaginary grounded cathode, as introduced in the equivalent circuit. However, the detailed origins of charge injection are still needed to be clarified from the viewpoints of physics. The concentration gradient of positive charges on both side of the double-layer elements will assist hole diffusion into the double-layer elements, due to the rather high holes mobility of the pentacene film, when charges are allowed to enter from the electrode. Meanwhile, it is known that there are many free negative ions in the open air and positively charged metals are thus discharged fast in the open air [20]. Accordingly, it is quite possible that negative ions in the open air serve to induce a potential drop between IZO and Al. Also the established potential across the double-layer element soon relaxes due to the displacement of the contact-generated holes through the C_{60} layer. As illustrated in Fig. 2(c), positive charges finally accumulate on the both IZO and Al electrode of double-layer elements. Consequently, the EFISHG signal decreased quickly after it reached the maximum value (see Fig. 2(a)). After the separation motion, the polyimide film was contacted with the Cu foil again. Negative charges on the polyimide film will be neutralized by positive charges induced on the Cu foil as well as on the connected IZO. In this situation, residual holes near the Al electrode will be attracted to the interface between contacted Cu foil and the polyimide film, which led to a negative potential drop pointing from the Al to the IZO electrodes. As shown in Fig. 2(a), the EFISHG intensity decreased firstly during the contact motion and then returned to the original level. This change of the EFISHG signal is the retrieve process of the residual charges in the double-layer element (see Fig. 2(c)), since the dielectric performance of the double-layer element can maintain the injected charges during the separation motion. After the residual charges transported through the C_{60} layer, the decreased EFISHG signal returned to the original level.

The equivalent circuit of double-layer element under the Al-Cu connection was also analyzed in a similar manner, on the basis of the Maxwell-Wagner model (see Fig. 2(d)). The EFISHG signal observed in Fig. 2(b) is nearly constant, and shows negligible change during both separation and contact motions, as illustrated in Fig. 2(d). In the separation motion, hole injection does not happen from the Al electrode, which is possibly due to the high injection barrier of Al electrode for holes. This phenomenon can be anticipated based on the injection characteristic of the double-layer element. However, it is interesting to find that in the succeeding contact motion, there is still no significant carrier behavior inside double-layer element, while the electron injection from Al side is possible. This stable SHG signal suggested that unlike the positive charges on Cu foil, CE-induced electrons on the surface of polyimide film is hard to move freely since the polyimide film is good insulator and these

charges are trapped near the surface of polyimide with a penetration depth of few nanometers [16, 17]. These results can be confirmed by the fact that the negatively charged film is not so easy to be discharged in the air [20]. Accordingly, as illustrated in the equivalent circuit of Fig. 2(d), the IZO side of double-layer element is electrically open-circuited in the air. These distinct carrier behaviors also showed us how the photovoltaic device reacts to the electrostatic interference induced by CE effect, which may help us to better preserve the devices. Meanwhile, the underlying carrier mechanism can also help us to better integrate the solar cell and the CE based energy harvesting device, such as TENG.

Furthermore, we have done some control experiment to further confirm the phenomenon. Firstly, in order to confirm the hole migration across the OSCs detected by the EFISHG, we performed an experiment by applying continuous contact-separation motion to the TENG device. The results can be seen in Fig. S4, where a series of peak signals can be detected by SHG observation. This experiment demonstrated the repeatability of the SHG measurements. On the other hand, in order to provide more straightforward evidence for this study, the OSC sample was replaced by a simple commercial LED with an operation voltage of 1.2 V, where the LED was also half suspended with a Cu-foil in the same way. During the CE process in the open air, the light was generated from the LED with the anode connected to the Cu foil, while there was no light emission when the cathode was connected to the Cu foil with both contact and separation motions. These results support our model in the fact that carriers are transported across the OSCs (and LEDs) with the Cu-IZO connection during the CE process, but not with the Cu-Al connection. Meanwhile, if the LED was placed in the vacuum, there is no light emission from it with either Cu-IZO connection or Cu-Al connection, which proved the contribution of the air. It is important to point out that the SHG measurement has some uncertainties for the quantitative analysis of the local electric field, since it is using laser signal to indirectly estimate the electric field. In contrast, the electrical measurements, such as multimeter, can directly read the voltage or current signal and these measurements usually offer more accurate results. However, the experimental flexibility of the SHG measurement can allow this technique to qualitatively study various special physical phenomenon. The detailed explanation of the advantage and uncertainties of the SHG measurement in comparison with common electrical measurement can be found in our recent work [21]. By coupling the SHG technique with some electrical measurement, we can get a more clear physics picture of the CE-induced carrier behavior.

Illumination was also applied to the double-layer element and the related contact-induced carrier behaviors have been probed by using EFISHG system, as shown in Fig. 3. In Figure 3, the double-layer element was in the

IZO-Cu connection mode and the response of the EFISHG signal was found similar to that under the dark condition (see Fig. 2(a)). The baseline of the SHG signal increased a little bit, which is due to the photovoltaic effect induced in the double-layer element. The changing amplitude (peak height) of the EFISHG signal was suppressed in comparison with the dark condition, which was due to the photoconductivity effect. Our previous study suggests that the established E_s is determined by the conductivity difference between two organic layers [10, 12]. Hence, the illumination leads to the increase of the d. c. conductivity of double-layer elements, and results in the faster diffusion of charges and the decrease of the established electric field. Results show that the CE effect and photovoltaic effect appear simultaneously without strong interaction or mutual influence, but the CE induced carrier behavior is affected by the illumination due to the contribution of photoconductivity.

4. Conclusion

By applying the EFISHG measurement to the half suspended double-layer photovoltaic element, we directly observed the variation of the internal electric field of double-layer elements under the excitation from CE effect, where one of the double-layer element's electrodes encountered with electrification and the other electrode was electrically isolated in the air. The charge injection happened only with the IZO-Cu connection. Meanwhile, no obvious change of internal electric field was observed with Al-Cu connection. The underlying mechanism of these carrier behaviors was analyzed based on the Maxwell-Wagner model. The study of this half isolated device offered us a physics picture about the photovoltaic device in response to the electrostatic phenomena induced by CE effect, which will be helpful for better utilizing solar cells and hybrid energy system consisted by solar cell and TENG. Finally, the EFISHG technique has been demonstrated to be an effective method for studying these CE related phenomena.

Acknowledgements

Thanks for the support from the "thousands talents" program for pioneer researcher and his innovation team, China; National Natural Science Foundation of China (Grant No. 61405131), the financial support by NSFC (Grant No. 51432005) and Beijing City Committee of science and technology (Z131100006013004, Z131100006013005). This work was financially supported by a Grant-in-Aid for Scientific Research (S) (Grant No.22226007) from the Japan Society for the Promotion of Science (JSPS), Japan. X. Chen thanks to Prof. Zhong Lin Wang (Beijing Institute of Nanoenergy and Nanosystems) for his guidance on the manuscript.

References

- [1] G. Zhu, J. Chen, T. Zhang, Q. Jing, Z. L. Wang, *Nat. Commun.* 5 (2014) 3426.
- [2] J. Bae, J. Lee, S. Kim, J. Ha, B. S. Lee, Y. Park, C. Choong, J. B. Kim, Z. L. Wang, H.Y. Kim, J.J. Park, U. I. Chung, *Nat. Commun.* 5 (2014) 4929.
- [3] Y. Xie, S. Wang, S. Niu, L. Lin, Q. Jing, J. Yang, Z. Wu, Z. L. Wang, *Adv. Mater.* 26 (2014) 6599.
- [4] X. Chen, M. Iwamoto, Z. Shi, L. Zhang, Z. L. Wang, *Adv. Funct. Mater.* 25 (2015) 739.
- [5] L. Zheng, Z. H. Lin, G. Cheng, W. Wu, X. Wen, S. Lee, Z. L. Wang, *Nano Energy* 9 (2014) 291.
- [6] L. Zheng, G. Cheng, J. Chen, L. Lin, J. Wang, Y. Liu, H. Li, Z. L. Wang, *Adv. Energy Mater.* (2015) doi: 10.1002/aenm.201501152
- [7] G. Cheng, L. Zheng, Z. H. Lin, J. Yang, Z. L. Du, Z. L. Wang, *Adv. Energy Mater.* 5 (2015) 1401452.
- [8] W. Seung, M. K. Gupta, K. Y. Lee, K.-S. Shin, J.-H. Lee, T. Y. Kim, S. Kim, J. Lin, J. H. Kim, S.-W. Kim, *ACS Nano* 9 (2015) 3501.
- [9] G. C. Yoon, K. S. Shin, M. K. Gupta, K. Y. Lee, J. H. Lee, Z. L. Wang, S.-W. Kim, *Nano Energy* 12 (2015) 547.
- [10] X. Chen, D. Taguchi, T. Manaka, M. Iwamoto, *Org. Electron.* 15 (2014) 162.
- [11] X. Chen, D. Taguchi, T. Manaka, M. Iwamoto, *Org. Electron.* 15 (2014) 2014.
- [12] X. Chen, D. Taguchi, K. Lee, T. Manaka, M. Iwamoto, *Chem. Phys. Lett.* 511 (2011) 491.
- [13] S. Niu, Y. Liu, X. Chen, S. Wang, Y. S. Zhou, L. Lin, Y. Xie, Z. L. Wang, *Nano Energy* 12 (2015) 760.
- [14] S. Niu, Y. Liu, S. Wang, L. Lin, Y. S. Zhou, Y. Hu, Z. L. Wang, *Adv. Funct. Mater.* 24 (2014) 3332.
- [15] S. Niu, Y. S. Zhou, S. Wang, Y. Liu, L. Lin, Y. Bando, Z. L. Wang, *Nano Energy* 8 (2014) 150.
- [16] E. Itoh, M. Iwamoto, *J. Appl. Phys.* 81 (1997) 1790.
- [17] M. Iwamoto, A. Fukuda, E. Itoh, *J. Appl. Phys.* 75 (1994) 1607.
- [18] T. Manaka, E. Lim, R. Tamura, M. Iwamoto, *Nat. Photonics* 1 (2007) 581.
- [19] Y. R. Shen, *The Principle of Nonlinear Optics*, Wiley, New York, 1984.
- [20] S. Wang, Y. Xie, S. Niu, L. Lin, C. Liu, Y.S. Zhou, Z. L. Wang, *Adv. Mater.* 26 (2014) 6720.
- [21] X. Chen, D. Taguchi, T. Manaka, M. Iwamoto, Z. L. Wang, *Sci. Rep.* 5 (2015) 13019.
- [22] See supplementary material at [URL will be inserted by CPL] for detailed analysis of physical model and the I-V measured by multimeter.

Figure captions

Figure 1. (a) Sample structure and the related experiment set up (b) I-V characteristics of the IZO/pentacene/C₆₀/Al sample in dark and illuminated conditions. (c) Maxwell-Wagner type theoretical model for the double layer sample.

Figure 2. (a) The EFISHG results from the contact triggered double-layer sample in dark, where the IZO electrode was connected to the Cu foil. (b) The EFISHG results from the contact triggered sample in dark, where the Al electrode was connected to the Cu foil. (c) The equivalent circuit of the sample under IZO-Cu connection during both separation and contact motion. (d) The equivalent circuit of the sample under Al-Cu connection during both separation and contact motion.

Figure 3. The EFISHG results from the contact triggered sample under illumination, where the IZO electrode was connected to the Cu foil.

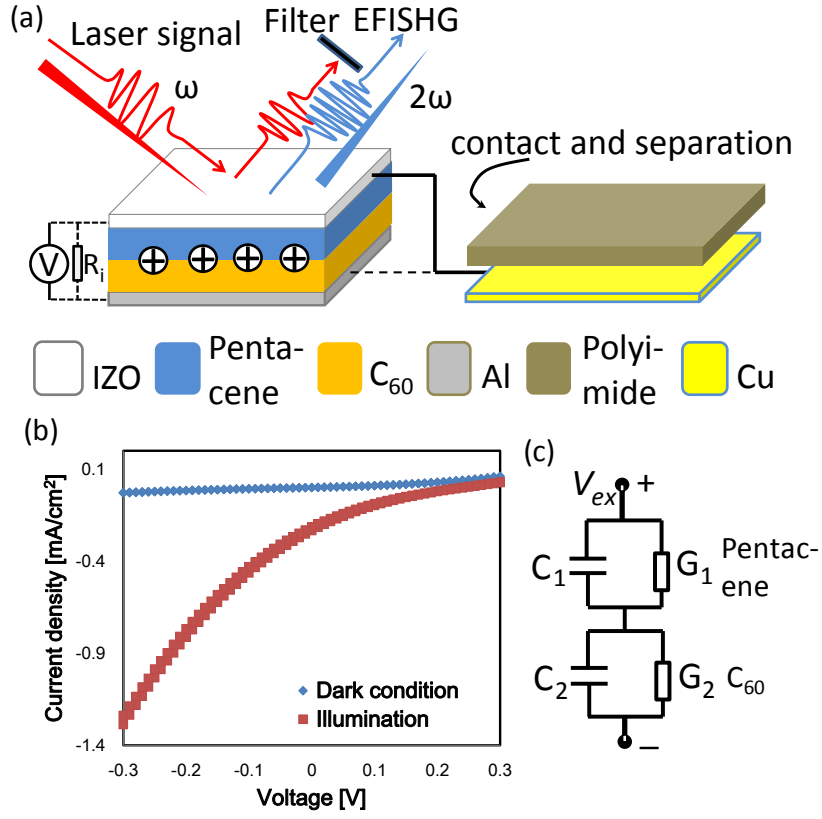


Figure 1. (a) Sample structure and the related experiment set up (b) I-V characteristics of the IZO/pentacene/ C_{60} /Al sample in dark and illuminated conditions. (c) Maxwell-Wagner type theoretical model for the double layer sample.

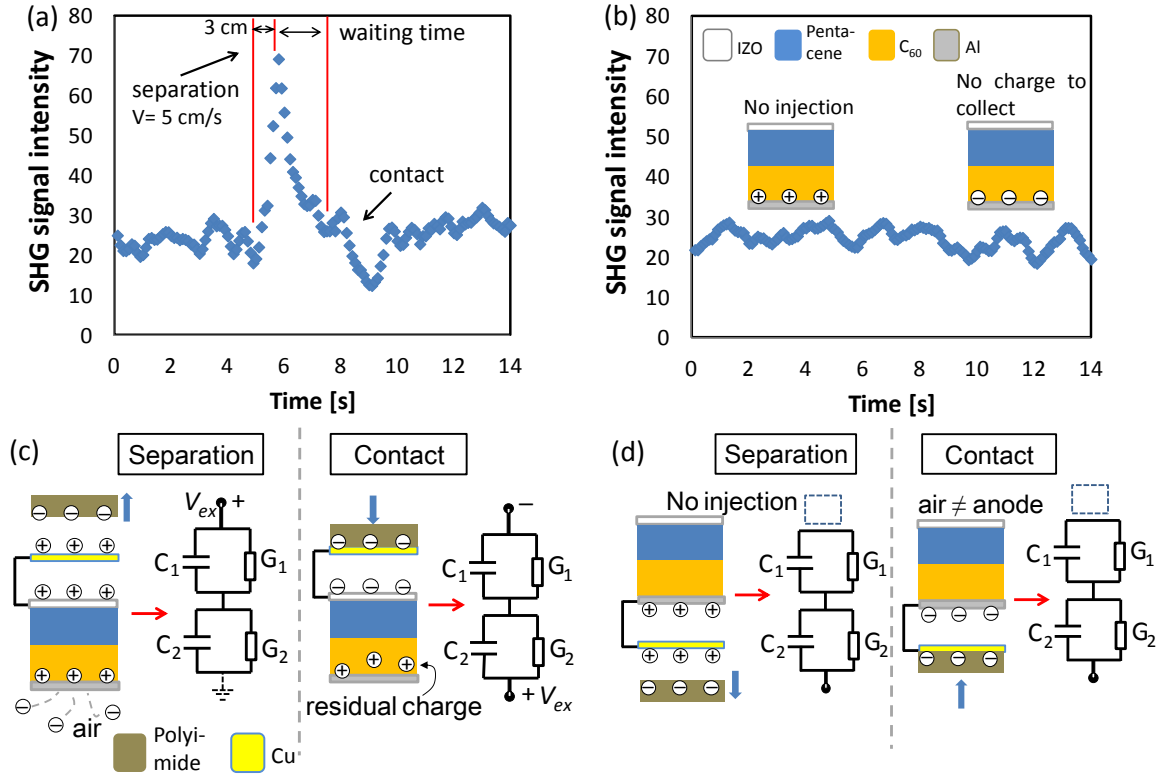


Figure 2. (a) The EFISHG results from the contact triggered double-layer sample in dark, where the IZO electrode was connected to the Cu foil. (b) The EFISHG results from the contact triggered sample in dark, where the Al electrode was connected to the Cu foil. (c) The equivalent circuit of the sample under IZO-Cu connection during both separation and contact motion. (d) The equivalent circuit of the sample under Al-Cu connection during both separation and contact motion.

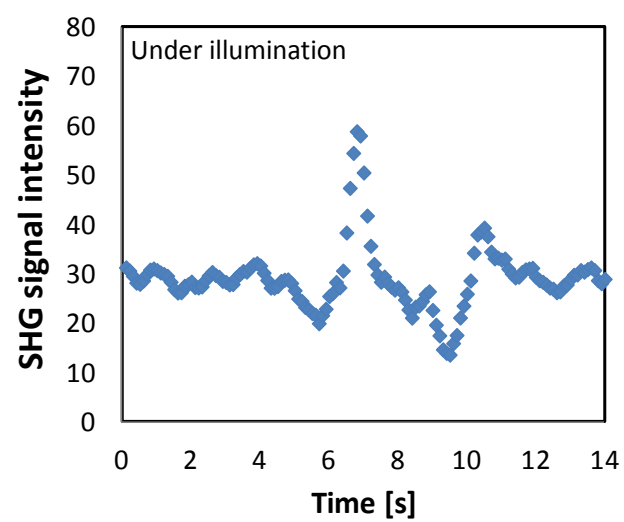


Figure 3. The EFISHG results from the contact triggered sample under illumination, where the IZO electrode was connected to the Cu foil.